values is ~3 dB for the EH_{11s} mode. This is not an unexpected result for the reasons already discussed.

Conclusions: We report the results of our measurements of the RCS of dielectric bodies of high permittivity. It is concluded that the resonant scattering cross-section of the electric or magnetic dipole modes of dielectric bodies of high permittivity can be computed with great accuracy using a very simple formula predicted by the asymptotic theory.

R. K. Mongia (*Department of Electrical Engineering, University of Ottawa, 161 Louis Pasteur, Ottawa, ON, K1N 6N5, Canada*)

C. L. Larose and S. R. Mishra (*David Florida Laboratory, Canadian Space Agency, Ottawa, ON, K1A 0Z4, Canada*)

P. Bhartia (*Defence Research Establishment Ottawa, Ottawa, ON, K1A 0Z4, Canada*)

References

1 VAN BLADEL, J.: 'On the resonances of a dielectric resonators of very high permittivity', *IEEE Trans.*, 1975, MTT-23, pp. 199–208
2 VAN BLADEL, J.: 'The excitation of dielectric resonators of very high permittivity', *IEEE Trans.*, 1975, MTT-23, pp. 208–215
3 MONGIA, R. K.: 'Theoretical and experimental investigations on rectangular dielectric resonators', *IEE Proc. H.*, 1992, 139, pp. 98–104

REALISATION OF FREQUENCY SELECTIVE HORN ANTENNA INCITED FROM PASSIVE ARRAY

J. C. Vardaxoglou, R. D. Seager and A. J. Robinson

Indexing terms: Horn antennas, Antennas, Frequency selective surfaces

A frequency selective horn prototype employing double-square array elements has been assessed experimentally. Results are shown which indicate that the concept will allow colocation of several high performance feed horns for integrated multiband operation.

The horn antenna described in this Letter is based on a concept presented in Reference 1 which shows that frequency selective surfaces (FSSs) may be used to guide EM energy by acting as frequency-dependent walls. Although this has been demonstrated in waveguide, a natural extension of the guidance is achieved by flaring out the array structure thus producing a frequency selective horn (FSH) antenna. A dual/multiband horn could be made by using two or more FSHs, of different size, mounted coaxially. Alternatively the outer horn could be solid metal as with traditional horns, and the inner horn an FSH. At low frequencies the inner FSH is transparent, and the effective horn dimensions are determined by the outer copper wall or outer FSH at resonance. At higher frequencies the inner FSH becomes opaque (reflecting) and guides energy as demonstrated later. Hence the outer structure becomes irrelevant and the device performance is dictated by the dimensions of the inner horn. The band separation is primarily dictated by the resonance frequencies of the coaxial FSHs and, inevitably, by the coupling between them. For large band spacings, we have two horns, colocated, each of which will ideally perform in the absence of the other, resulting in a high performance dual/multiband integrated horn.

We present the performance of a single conical FSH prototype which was constructed by simply folding a planar sector of an etched surface into a cone (Fig. 1a). The sector angle α_c is 80° and the lengths L_c and L_T are 16 and 19·4 cm, respectively. A double-square element geometry was used [2, 3]. The side length f the inner square is $l_i = 3\cdot1$ mm and the outer side length $l_0 = 5\cdot2$ mm. The widths of the inner and outer squares were 0·1 and 0·7 mm, respectively. The array elements

were arranged on a closely packed square lattice of side $D = 5\cdot5$ mm and printed on a 0·05 mm thick dielectric substrate ($\varepsilon_r = 3$). The surface was glued to a 0·1 mm thick acetate former ($\varepsilon_r \approx 2\cdot33$) to provide rigidity. Fig. 1b shows the cross-section of the FSH whose semiflare angle $\alpha_s \approx 12\cdot8°$, length $L = 15\cdot6$ cm and aperture radius $d = 4\cdot4$ cm. The horn surface area was 0·025 m² which accommodated over 840 conducting elements. The mechanical properties of the cone were such that when its apex was inserted into the open end of a waveguide, the profile of the surface contained a smooth transition from rectangular to circular cross-section. A solid (nonpatterned) horn was also made in the same way from flexible dielectric-backed copper sheet. Copolar and cross-polar pattern measurements were performed in the principal and 45° planes of the FSH and these were compared with results obtained from a solid copper horn and an open ended waveguide response. The electric field of the waveguide was taken parallel to y_h and the sector axis y was in the $y_h - z_h$ plane. As a consequence of using a square lattice, the array elements are oriented at varying angles to the boresight axis at different positions of the curved surface.
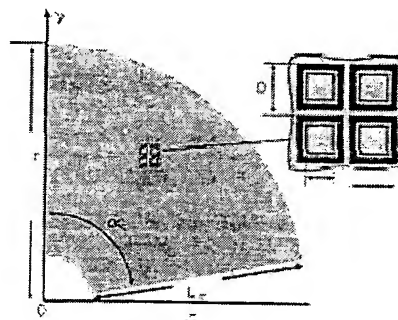

Fig. 1 *Top view of planar sector showing geometry and orientation of double-square array and cross-section of conical frequency selective horn depicting the array*

a Top view
b Cross-section

Fig. 2 shows the boresight frequency response of the FSH compared with that of the copper horn and open ended waveguide. It may be seen that near the array resonance (around 15 GHz) the gain of the horn approaches that of the copper horn, indicating that at this frequency the FSH walls are indeed acting as good reflectors. In the absence of the dielectrics the wavelength of the resonance is approximately equal to the circumference of the outer square giving 15·5 GHz. Away from the resonance the response approaches that of the open waveguide, indicating that the walls are becoming inert. According to the approximate directivity formula [4] for a solid horn, $10 \log_{10}(2\pi d/\lambda)^2 - (0\cdot8 - 1\cdot71s + 26\cdot25s^2 - 17\cdot79s^3)$, where the maximum phase deviation $s = (d^2/2\lambda L_c)$, the gain at 14·5 GHz is 21 dBi. At the same frequency the measured gain of the FSH is ~19 dBi. This decrease is partly due to the lossy adhesive used and partly due to the discontinuity mismatches of the array along the line joining the sector in the FSH construction. Also shown in Fig. 2 is the measured plane wave transmission response for normal incidence of a 20 cm square flat array. As expected, the

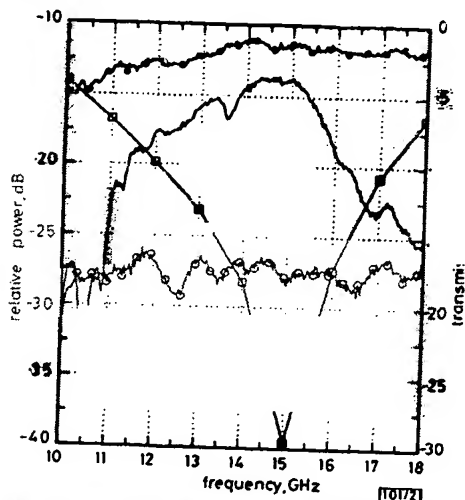reflection band centre is broadly coincident with the FSH band centre.

Fig. 2 *Frequency response comparison (forward transmission) of FSH, solid horn and open ended waveguide*

———— FSH
—●— solid horn
—⊖— open ended waveguide
—□— flat array plane wave transmission (right y axis)

Fig. 3 shows the H-plane radiation patterns for the FSS horn, solid copper horn and open waveguide at 14·5 GHz. There is good correlation between the FSH and solid horn patterns with the exception of a slight beam squint and a minor sidelobe degradation beyond ±30° of azimuth. Similar comments apply to the comparison in the E plane and 45° plane. Peak crosspolar levels of ~ −22 dB were observed in the E and H planes. In the 45° plane the peak crosspolar level reached −18 dB, which is not unreasonable considering the wide variation of local incidence on the elements as well as the array asymmetry resulting from laying a square lattice onto a conical surface.

It has been shown that it is possible to devise a microwave horn antenna using conventional passive arrays as frequency
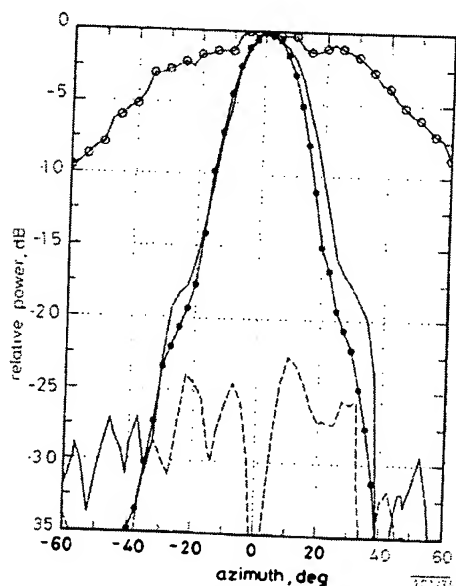

Fig. 3 *H-plane radiation patterns at 14·5 GHz*

———— FSH copolar
- - - - FSH crosspolar
—●— solid horn
—⊖— open ended waveguide

1956

dependent walls. Such an FSH has been simply made and tested, and, at resonance, its performance has been found to be similar to that of a comparable horn made with contiguous copper sheet. Away from resonance, the performance reverts to that of the open waveguide. This opens up possibilities for designing novel broadband or multiband horns using several coaxially mounted FSHs with different resonance frequencies. To achieve this, however, we need to investigate fully the mode content of the fields in and around the aperture of the FSHs adopting modal techniques used to analyse multilayer surfaces [5], as well as tailoring the array geometry to fit the horn curvature.

J. C. Vardaxoglou, R. D. Seager and A. J. Robinson (*Department of Electronic and Electrical Engineering, University of Technology, Loughborough, Leicestershire LE11 3TU, United Kingdom*)

References

1   VARDAXOGLOU, J. C., SEAGER, R. D., and ROBINSON, A. J.: 'Waveguide and aperture antenna including frequency selective surfaces'. International Patent, 1992, Filing No. PCT/GB92/01173
2   LANGLEY, R. J., and PARKER, E. A.: 'Double-square frequency selective surfaces and their equivalent circuit', *Electron. Lett.*, 1983, 19, pp. 675–677
3   VARDAXOGLOU, J. C., and STYLIANOU, A.: 'Modal analysis of double-square frequency selective surfaces'. Proc. Int. Conf. in Electromagnetics on Aerospace Applications, ICEAA, 1989, Torino, Italy, pp. 355–358
4   JASIK, H. (Ed.): 'Antenna engineering handbook' (McGraw-Hill, New York, 1961)
5   STYLIANOU, A., DEBONO, P., and VARDAXOGLOU, J. C.: 'Iterative computation of current and field distributions in multi-layer frequency selective surfaces', *IEE Proc. H.*, 1992 (in press)

EFFECT OF F1-LAYER L CONDITION ON RANGING ACCURACY FOR SSL HFDF SYSTEMS

D. C. Baker and J. J. Burden

An extension of the multisegmented quasiparabolic model of ionospheric electron density to include the F1-layer L condition is described. Provisional results illustrating the effects of this on ranging estimates from single station location HFDF systems are discussed. It is concluded that a knowledge of actual ionospheric conditions at the time of observation are important for such systems to improve ranging estimates, especially when L conditions are present.

Introduction: The multisegmented quasiparabolic (MQP) model of ionospheric electron density distribution was developed independently by Baker and Lambert [1, 2] and Dyson and Bennett [3]. A description of the use of this model for single station location (SSL) HFDF systems is given by McNamara [4]. The MQP model has been enhanced to include the effect of the geomagnetic field [5], and the multisegmented parabolic (MP) version to incorporate the F1-layer L condition [6]. This Letter describes a modification of the MQP model to include the L condition and illustrates the effect of this condition on ground range estimates in SSL HFDF systems.

Extension of MQP model: In the MQP model the electron density distribution $N(r)$ is given by equations of the form

$$N(r) = a \mp b(r - r_m)^2(r_b/r)^2 \qquad (1)$$